CFD ANALYSIS OF GAS EXPLOSIONS VENTED THROUGH RELIEF DUCTS: THE EFFECT OF THE DUCT GEOMETRY

Ferrara G.[1],*, Di Benedetto A.[2], Salzano E.[2], Russo G.[1]
[1] Dipartimento di Ingegneria Chimica, Università "Federico II", Napoli
[2]CNR-IRC, P.le Tecchio 80, 80125 Napoli
***g.ferrara@irc.na.cnr.it**

ABSTRACT

Venting devices are commonplace and cheap solution in industrial installations for the mitigation of accidental explosion. Quite often, fitting relief ducts to vent openings is mandatory in order to discharge combustion products to safe location. However, the presence of the duct is likely to increase the severity of the explosion with respect to simply vented vessels posing a problem for the proper design of this venting configuration. Several mechanisms have been proposed to account for the enhanced violence of the explosion in such a venting configuration but uncertainty still stands. The lack of both investigation and comprehension has so far prevented the development of reliable engineering guidelines for the sizing of the vent area. In this work a numerical tool based on a CFD model is used to study the effect of the vent area and duct length on the over-pressure reached in the main vessel. Experimentally observed trends are discussed with the aid of the numerical results and practical implications of the role played by the duct geometry (length and diameter of the duct) are addressed.

1. INTRODUCTION

Vent devices for gas and dust explosions are often ducted to safe locations by means of relief pipes, for the discharge of hot combustion products – possibly toxic – or blast waves [1,2]. Relief pipes are specifically required when the hot jet flowing violently from the vent area has to be avoided, e.g. within buildings. On the other hand, the presence of a duct is likely to increase the severity of the explosion with respect to simply vented vessels [2-5].

In the last two decades a number of works have addressed the issue of gas explosions vented through relief pipes [4-9]. Several phenomena were identified as affecting the increase of the overpressure with respect to simply vented vessels such as secondary explosion in the duct (burn-up), frictional drag and inertia of the gas column in the duct, acoustic and Helmholtz oscillations.

Acoustic oscillations are deemed to be involved in the generation of later strong pressure peaks in simply vented vessels [10]. Kordylevski & Wach [7] detected acoustic oscillations in the pressure records of their experiments on small-scale ducted vent explosions suggesting this phenomenon could be somehow responsible for the unusual pressure rise in the vessel. Actually the link was quite loose as they observed stronger pressure rises (with respect to simply vented vessels) also in the absence of oscillatory behaviour. Moreover, Ponizy and Leyer [5] reported an increased violence of the duct-vented explosion on a small scale with stoichiometric propane-air mixtures which does not constitute a suitable condition for acoustic enhancement of explosion [11].

Helmholtz oscillations in small explosion chambers fitted to venting ducts were observed early by Cubbage and Marshall [12]. Also, McCann et al. [13] clearly detected Helmholtz oscillations in the final stages of explosions in small scale vessels fitted to duct of different lengths. They pointed out that such oscillations could play an important role in triggering Taylor instability. Nevertheless, this effect cannot be considered necessary condition for the increase of the explosion violence, as the occurrence of this flame front instability is well acknowledged even in simply vented vessels [14]. Besides, as pointed out by the same authors, such oscillations should have more pronounced effects on larger scale explosions as confirmed by Kumar et al. [15], who detected severe Helmholtz type oscillations for middle scale lean hydrogen-air explosions vented through a duct.

The turbulent mixing of hot and fresh gases in the initial section of the duct after the flame entrance promotes a violent burning therein (an explosion-like combustion or "burn up"). Hence, the pressure impulse in the duct induces the backflow of gases from the duct to the vessel with the possible consequent turbulization of residual combustion in the vessel and the blockage of the gas efflux [4,5]. This violent explosion in the duct named as burn up was addressed by some authors as the main responsible for the dramatic increase of the pressure in the vessel [4,5,9,16].

Other authors indicated additional pressure drops due to the resistance of the gas flow in the vessel-duct assembly as main responsible for the higher pressure rise in the vessel with respect to simply vented vessels [17,18]. Mechanical, steady-state type pressure drops for the present configuration can be substantial due to the very high flow velocities attained in the duct and the concentrated losses in the sudden flow area changes (respectively at the duct entrance and exit).

On the theoretical side, some efforts have been devoted to get insights into the phenomenon by developing mathematical models. Zero-dimensional models proved effective in advancing the comprehension and the formalization of data gained for simply vented explosions [19-21]. Zero-dimensional and one-dimensional models [4,17] were also proposed to represent an explosion vented through a duct but result in a scarce predictive capability as they rely strongly on empirical parameters. In fact, it could not be expected that such models provided a sound description of the phenomenon due to the assumption of a spherical flame propagation whatever the geometric complicacy (here included the presence of a discharging duct). According to these models the enhancement of the burning rate through turbulization [4] and the friction losses [17] are the most important phenomena affecting overpressure.

The available guidelines for the design of ducted vents for gas explosions are those proposed by Bartknecht [3], also reported in NFPA 68 [1], which gives a barely empirical correlation based on simply vented vessels indications presented in the same reference. Due to their empirical foundation, NFPA correlations are to be used very carefully as they can lead to gross errors [20].

Prior to any correlation development, a sensible approach should be trying to better understand the phenomenology of the whole explosion that, as shown, appears quite complex. This step appears to be preparatory (if not mandatory) for the selection of the ruling parameters and for the making of the necessary approximations aiming at developing sound engineering correlations.

To this regard it must be noticed that, when care is used in analyzing their results, CFD models can be valuable tools in assessing explosion scenarios provided that a satisfactory validation is carried out [22-26]. CFD models can in principle take into account much more physics than zero-dimensional models as they can, for example, relieve the severely restrictive hypothesis on the geometry of the system and of the propagating flame.

In this work a model previously developed [27], is exploited to obtain a better comprehension of some experimental trends observed on a laboratory scale [5,9]. Comparison of predictions with experimental data is presented and explanations of experimental observed trends are proposed on the basis of model results. More specifically, the effects of varying the duct geometry (length and diameter) have been studied and analysed with the aid of the numerical computations.

2. THE MODEL

The analysis of ducted vented explosion has been performed by means of a finite-volume CFD 2D axis-symmetric model based on the unsteady-RANS approach. The model is based on the Reynolds averaged mass, momentum and energy balance equations. The full set of the conservation equations is reported in [27] and has been numerically solved by means of the commercial general purpose CFD code CFD-ACE+ [28]. Reliability of RANS predictions strongly depends on reliability of sub-models used to describe the effects of combustion, turbulence and their interactions at the scales not resolved by the numerical grid. In the following the chosen turbulence and combustion models are described.

2.1 The turbulence model

In this work the *k-ε* model [29] has been used to model the turbulent flow. A number of shortcomings of *k-ε* models when applied to turbulent combustion problems are known and is generally accepted that more complex second moment Reynolds stress models should be able to describe more of the turbulence-combustion interaction [30]. Nevertheless, at least for the current level of development, the widespread use of second moment models is prevented by their lack of numerical robustness [22], which makes un-worthy their much higher computational cost with respect to traditional two-equations models.

Classical wall functions have been employed for the determination of the flow velocity in the viscous layer adjacent to the walls. To this regard is worth noticing that the use of wall functions is expected to give poor results in the region of flow separation and reattachment, at the duct entrance. Nevertheless, as this region is confined to a very small section at the beginning of the duct, modelling errors related to this choice have been deemed to be not dramatic [31].

2.2 The combustion model

The explosion phenomenon is intrinsically unsteady: starting from ignition in the first vessel, a laminar flame propagates. Due to the turbulence induced by gas expansion and interaction with geometry, in particular with the duct entrance section, transition from laminar flame to turbulent flame may occur trough different combustion regimes.

The starting point in the development of the combustion model was the lack of a universal expression for the averaged source terms valid in all the combustion regimes. To this aim the source term has been adapted at each time step referring to local non-dimensional quantities related to the flow and combustion characteristics (such as the ratio of the turbulent fluctuating velocity to the laminar burning velocity and the Karlovitz number). Different expressions have been used to allow for the different combustion regimes experienced during the explosion. Further details can be found in [27].

The combustion models were implemented in the CFD code by means of user-subroutines. Description of the chosen model for each regime follows.

2.2.1 Laminar flame propagation

A phenomenological approach has been used for the laminar phase propagation [32]:

$$\overline{\dot{\omega}} V_{cell} = Y_u \rho_u S_L A_F \tag{1}$$

where $\overline{\dot{\omega}}$ is the averaged rate of consumption of the fuel, Kg s^{-1}; V_{cell} is the volume of the computational cell, m^3; Y_u is the fuel mass fraction in the unburned gases; ρ_u is the density of the unburned gases, Kg m^{-3}; A_F is the flame area in the computational cell, m^2; S_L is the laminar burning velocity of the mixture, m s^{-1}. It is worth noticing that all CFD codes which rely on expressions like Eq. (1) to represent the laminar phase combustion [25,26], involve corrections and/or adjustable parameters to estimate the flame area. In the present work the flame area in each computational cell in the laminar phase has been calculated as:

$$A_F = \xi V_{cell}^{2/3} \tag{2}$$

where the constant ξ (= 5/3) has been evaluated by matching the calculated pressure curves in the laminar phase propagation with the experimental trend for a single test case reported in [5,9] as described in details in [27]. Any numerical test case reported in this work has been obtained by using the constant value of ξ reported above.

2.2.2 Flamelet combustion regime

Eddy Break Up models [33] and algebraic flamelet models [34] have been traditionally the most widely used in the numerical modelling of gas explosions due to their simplicity and low computational cost. Both these models involve an expression of the type:

$$\overline{\dot{\omega}} \propto \frac{1}{l_T} \tag{3}$$

where l_T is the local integral length of turbulence, m. Expressions like Eq. (3) lead to not bounded values for the burning rates when combustion spreads near walls as l_T approaches zero near solid surfaces. Due to the particular relevance of combustion into boundary layers in our configuration, a modified form of the algebraic flamelet expression has been used [35]. In this equation the turbulence length is replaced by a laminar length that preserves a finite value close to solid surfaces.

The general algebraic flamelet expression as proposed in Bray & Libby [34] is:

$$\overline{\dot{\omega}} = \rho_u S_L I_o \Sigma \tag{4}$$

where I_o is the "mean stretch factor", assumed to be unity in the present work and Σ is the flame area density (m^{-1}) expressed as:

$$\Sigma = g\frac{\overline{c}(1-\overline{c})}{\sigma_y L_y} = \frac{g}{\sigma_y L_y}\frac{1+\tau}{(1+\tau\widetilde{c})^2}\widetilde{c}(1-\widetilde{c}) \tag{5}$$

where the constants g and σ_y are respectively 1.5 and 0.5, τ is the heat release factor ($\tau = T_b/T_u - 1$) with T_u and T_b respectively the temperature in the unburned and burned gases, K; L_y is the characteristic flamelet length (m) expressed in the original version of the model as proportional to the integral turbulence length. In Abu-Orf and Cant [35] the expression for the flamelet length is expressed as a function of the characteristic laminar length l_L (m) and is fitted with an experimentally determined function f which returns the turbulent burning velocity as a function of the normalized *rms* velocity (u'/S_L):

$$L_y = C_L l_L f\left(\frac{u'}{S_L}\right) \tag{6}$$

where C_L is a non-dimensional model constant.

Another major issue of this expression is that the empirical function f allows the extension of the validity of the starting expression beyond the flamelet regime to regimes characterized by high strain rates. This characteristic has been of fundamental importance for our configuration as high strain rates and subsequent (temporary) flame quenching are attained in the first sections of the duct [36], thus playing a crucial role in the development of the whole combustion process. It is here important noticing that no adjustable parameter has been fitted in the modified flamelet expression to evaluate the turbulent cell flame area as this value is calculated by the model as a flame area density (Σ).

2.3 Numerical solution

Resolution of the discretised set of equations has been carried out by means of the SIMPLEC algorithm extended to compressible flows [37]. Pressure-correction methods, extended to allow for arbitrary Mach numbers, are effective in treating the viscous compressible fluid dynamic equations in both the high and low Mach number limits, which both occur in vented explosions.

A fully unstructured grid has been used to mesh the physical domain whose cylindrical shape has allowed the choice of a 2D-axysimmetric numerical domain (see Fig.1). Non uniform unstructured grids have been preferred to structured grids aiming at minimizing discretization errors [31] and at avoiding artificial preferential direction of flame [26]. Triangular cells have been used whose characteristic linear dimension (diagonal) lies in the range: $\Delta x = [10^{-3}, 10^{-2}$ m]. The most limiting issue for the selection of the time step has resulted the stability of the numerical solution that has eventually limited it in the interval $\Delta t = [10^{-5}, 10^{-4}$ s]. The presence of the steep temperature and progress variable gradients at the flame front together with severe gradients of flow velocity and turbulent variables in the boundary layers, has led to the choice of first order upwind differences in the spatial discretization scheme for all the variables in order to avoid numerical instabilities of the computed solutions.

The accuracy of the numerical solutions has been checked by studying three mesh sizes obtained by refining a starting grid: the finer grids have been obtained reducing the cell size of the coarse starting grid (about 12000 cells). Discretization error has been estimated to be lower than 10% on the finest grid (about 48000 cells) and about 20% on the coarsest grid (percentage is referred to the estimated exact numerical solution). This difference has been deemed to be not dramatic for the purposes of the present work and all calculations have then been carried out on the intermediate refined grid.

Numerical computations have been carried out on a parallel cluster employing 8 processors AMD Opteron 200 (2.4 GHz). Run-times were approximately 6 hours for the intermediate grid (24000 cells).

2.4 Experimental setup

Validation of the model has been addressed by comparison with the experimental results obtained by Ponizy & Leyer [5]. They reported tests carried out in a cylindrical vessel of fixed volume ($V = 0.0036$ m^3) connected to a coaxial cylindrical duct. A sketch of the base case experimental set-up is shown in Fig.1, where the experimental monitor points corresponding to numerical monitor points, for the sake of comparison, are also reported.

Experiments were performed for propane-air stoichiometric mixtures ($Y_u = 4.0\%$ vol.) and by varying the tube length L_t, the duct diameter D_t and the ignition position (either in the geometrical center of the main vessel or in the rear side, opposite to duct entrance). Initial conditions consisted in atmospheric pressure and temperature for all performed test.

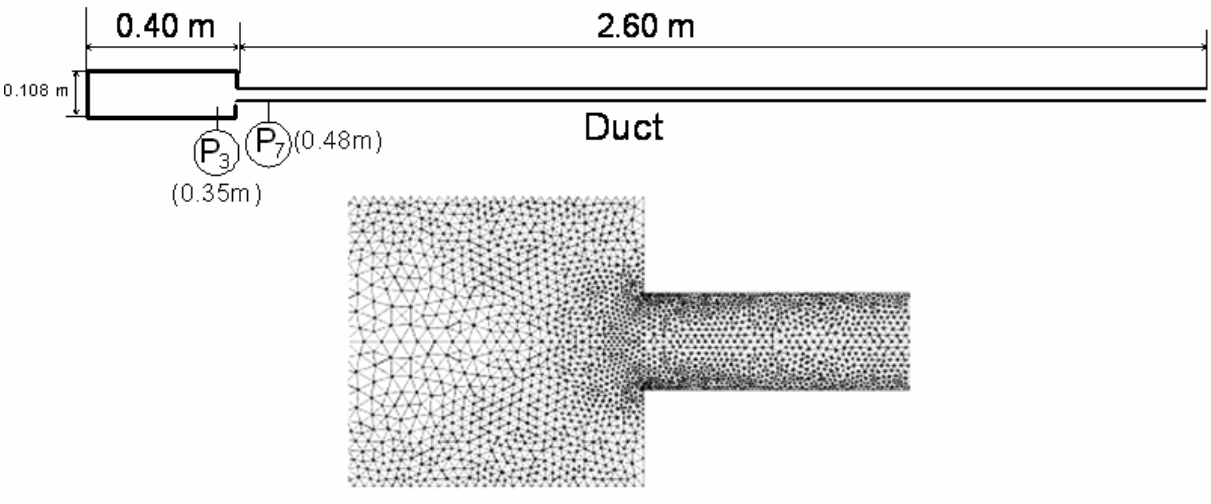

Figure 1 – Sketch of the experimental setup and detail of the computational grid.

3. RESULTS AND DISCUSSION

Comparison between experimental and numerical data together with validation issues, have been previously reported [27]. It is here worth to remark that the agreement between model and experimental results has proved satisfactory standing the ability of the model to reproduce both the pressure history, a global variable, and, more effectively, the dynamics of flame propagation. Hence, the numerical results have been deemed suitable in assessing the effect of the duct geometry on the explosion behaviour.

3.1 Effect of duct length

The effect of the duct length on explosions vented through relief pipes was extensively studied in the literature [3,5-7,38] allowing to establish quite a clear trend. The maximum pressure experiences a very rapid increase with the initial increase of the duct length, while increasing (or even decreasing) with lower rates as the duct length is further increased. Effects related to the duct length were traditionally dealt with guessing a role for the additional pressure drops related to the presence of the duct [3,18]. Indeed, as already mentioned, the flow resistance in the vessel-duct assembly causes a pressure drop that adds to the combustion- related pressure rise in the vessel.

Ponizy and Leyer [5,9] carried out tests varying the duct length between 0.6 and 2.6 m. In Figure 2 the comparison between model and experimental results for a 0.036 m duct diameter is reported. Both the experimental and the model data show an increasing trend as function of the duct length. Numerical results have been used to gain some insights into the shape of the maximum pressure in the vessel as a function of the duct length trying to ascertain the role of purely mechanical pressure drops. Calculated flow gas velocities (averaged values along the duct axis) have been collected for the various duct lengths aiming at estimating the additional pressure drops due to the presence of the duct. Fig.2 reports the evaluated pressure drops as a function of the duct length relative to instants following the burn-up. Steady state pressure drops have been evaluated by means of Eq. (7):

$$\Delta P_{steady} = \Delta P_{in} + \Delta P_{duct} + \Delta P_{out} = \frac{1}{2}\rho u^2 \left(K_{in} + 4F\frac{L_t}{D_t} + K_{out} \right) \tag{7}$$

where ΔP_{steady} is the overall pressure loss across the duct, bar; ΔP_{in} and ΔP_{out} are the concentrated pressure losses at the duct entrance and exit, ΔP_{duct} is the distributed pressure loss along the duct, u is the velocity of gases, m s^{-1}; K_{in} and K_{out} are respectively the pressure loss coefficients for a sudden flow area restriction and a sudden flow area enlargement (compressibility effects have been taken into account using values suggested in Benedict et al. [39]), F is the friction factor for the flow in the duct evaluated from traditional relationships [40].

In Figure 2 the pressure drop calculated according to Eq. (7) and the difference between the peak pressure in the vessel in the presence of the duct and that in the corresponding ductless vessel ($P_{3,max}$ = 0.9 bar g) are plotted versus the duct length. It is worth noting that the order of magnitude of these pressure differences is the same suggesting that the effect of length is mainly related to the pressure drop. As a consequence by increasing the duct length, the overpressure in the vessel is increased according to the pressure drop.

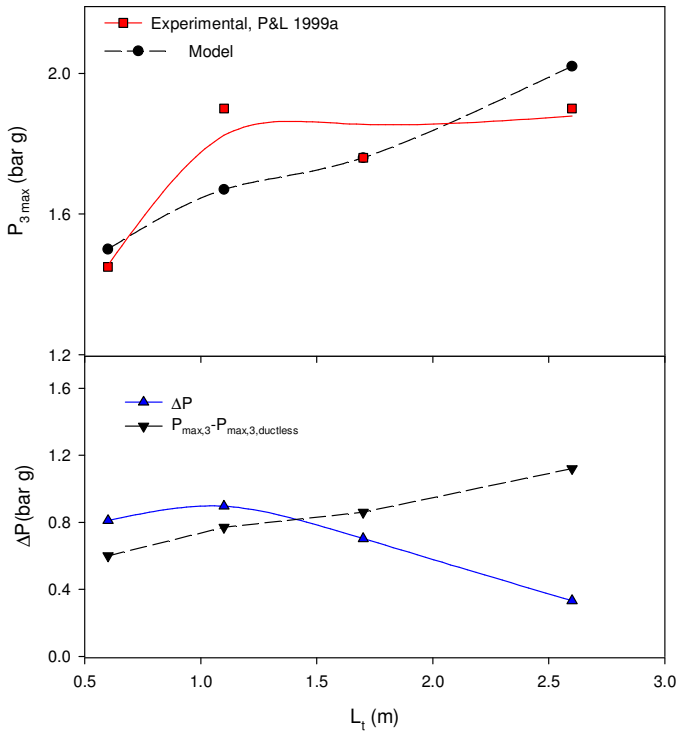

Figure 2- Duct length effect. Comparison between calculated and experimental maximum pressure in the vessel as a function of duct length; comparison between calculated pressure drops and duct related pressure rise in the vessel ($P_{3,max}$ - $P_{3,max}$,ductless vs L_t) following burn-up effects.

.

3.2 Effect of diameter

The effect of vent area on the maximum pressure reached in a simply vented gas explosion has been thoroughly investigated [41,20]. Analysis of comprehensive data collection in such works allowed to derive empirical correlations reporting an always monotonic decrease of the maximum pressure with vent area. To the authors' knowledge, vent area effects for gas explosions vented through relief pipes has been addressed only by Ponizy and Leyer [5,9] and Molkov [4].

An interesting issue is shown in the paper of Ponizy & Leyer [5] as the vessel overpressure displays a non monotonic behaviour with respect to the vent area (i.e. the duct diameter). In particular the maximum pressure was observed to exhibit a minimum in correspondence of an intermediate value of the duct diameter for all the investigated duct lengths.

In the present work, the experimental results of Ponizy and Leyer [5] for a 1.1 m duct length and three duct diameters (0.016 m, 0.021 m, 0.036 m), have been numerically reproduced. Table 1 displays the comparison between numerical and experimental data for the maximum pressure recorded in the vessel revealing a good agreement. It is noticeable the capability of the model to capture the non-monotonic trend of the maximum pressures.

It is well known that the peak pressure reached in a vented vessel (P_{max}) is the outcome of a competition between the combustion rate and the venting rate that, following Molkov [19], can be formalized as:

$$P_{\max} = \varphi\left(\frac{Combustion\ \ rate}{Venting\ \text{rate}}\right) \tag{8}$$

where φ is an analytically determined function. Numerical calculations have the potential to provide information on both quantities that feature Eq.(8) as a function of the vent area A_v (m^2) thus allowing to understand how the vent area affects the final pressure level recorded in the vessel. In particular, integrating the flow field on the cross section in correspondence of the vent area, it is possible to evaluate the venting rate $\dot{m}_v$ (Kg s^{-1}) at each time:

$$\dot{m}_v = \int_{A_v} \rho\, u\, dA_v \tag{9}$$

where ρu is the mass flux in the axial direction normal to the cross sectional vent area, Kg m^{-2} s^{-1}. Also, integrating the calculated source terms on the whole flame surface, it is possible to evaluate the wrinkling due to turbulence (χ):

$$\chi = \frac{wrinkled\ flame\ surface}{smooth\ surface} \tag{10}$$

The venting rate gives information on the venting effectiveness. The wrinkling factor is a measure of how effective are turbulent motions in increasing the flame area and then the overall burning rate. Values of χ higher than unity represent wrinkled flame surfaces.

Fig.3 reports the venting rates and the flame averaged enhancement factors (χ) as function of time, for the three diameters. In Fig.4 the propane mass fraction is shown for the three diameters in correspondence of the backflow time (i.e. when a burning rate enhancement is expected to occur in the vessel).

It can be seen that the flame propagation in the vessel vented through the smallest duct diameter (D_t = 0.016m) is almost un-disturbed with respect to the larger diameters. Indeed, from Fig.3 it is evident that the χ factor value is definitely lower than the other two. Also, from Fig.4, it appears that the flame shape is almost unaffected by the mild back-flow. If no substantial combustion enhancement is observed, the low venting effectiveness (Fig.3) must be considered responsible in determining the final pressure rise. Considering the intermediate diameter (D_t = 0.021), it can be seen that the maximum pressure is relieved due to the higher venting rate with respect to the smallest diameter (see Table 1).

Quite unexpectedly, the maximum pressure relative to the largest diameter (D_t =0.036) results in a higher value than the intermediate diameter even if the venting effectiveness is the highest between the three diameters (see Fig.3). If the venting rate is relatively effective, one must think to enhanced burning rates to explain for the pressure rise. To this regard, the wrinkling factor alone cannot explain for high burning rates as its value is lower than the one relative to the intermediate diameter (see Fig.3).

The substantial increase in the burning rate for the largest diameter is to be ascribed to the large flame deformation that characterize the interaction between the backflow and the residual combustion in the vessel for the largest diameter (Fig.4; D_t= 0.036m). The wrinkling factor for the largest diameter is close to the one observed for the intermediate one (Fig.3) but it acts on a flame surface that is almost twofold (see Fig. 4) thus resulting in a greater overall burning rate.

The non-monotonic trend can thus be explained as the outcome of the competition between the burning rate and the venting rate. Increasing the duct diameter is always accompanied with the increase of the venting rate, which tends to relieve the pressure in the vessel. On the other hand, larger

diameters also result in more pronounced flame distortions, thus promoting the pressure rise in the vessel.

Table 1 - Effect of diameter. Comparison between calculated and experimental values. P_3 is the pressure in the vessel; t_0 is the time of flame entrance into the duct.

Diameter [m]		**$P_{3,max}$ (bar g)**	**$P_{3,0}$ (bar g)**	**t_0 (s)**
0.016	Experiment	1.75	1.25	65
	Model	2.14	1.67	66.5
0.021	Experiment	1.4	0.9	51
	Model	1.55	1.1	51.3
0.036	Experiment	1.9	0.6	34.9
	Model	1.67	0.71	36.1

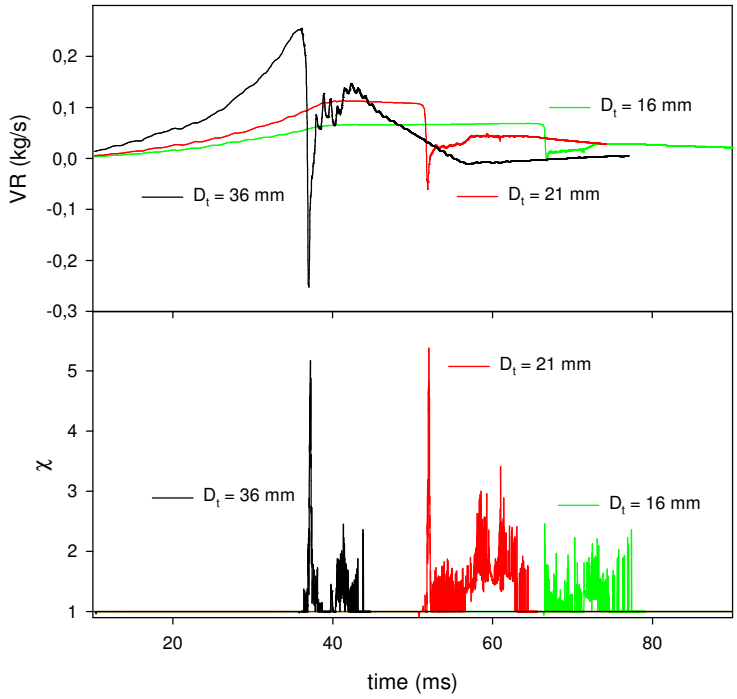

Figure 3 - Effect of diameter. Comparison between calculated venting rates and turbulent enhancement factors for different diameters.

The increase of the flame distortion as the vent area is augmented, explains for the increase of pressure and the non monotonic trend. Differently from what observed for simply vented vessels, when a duct is fitted to the vent the higher the vent area does not mean the lower the peak pressure.

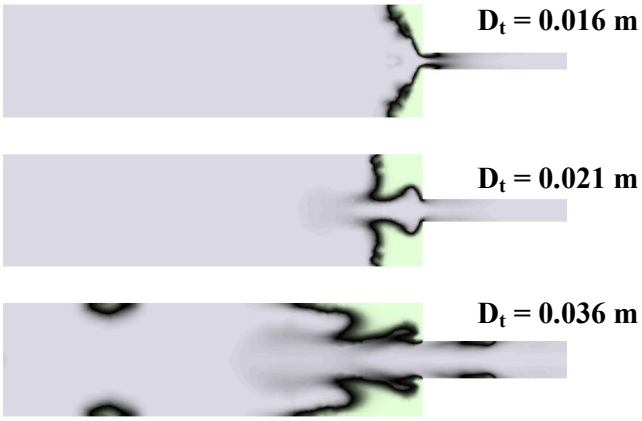

Figure 4 - Calculated propane mass fraction in the whole configuration at three values of duct diameter in correspondence of the backflow time.

While further study of the effect of the duct diameter is necessary on scales of industrial interest, it is here proposed that other strategies (water sprinklers or flame arresters in the initial sections of the duct) could be more effective than truly increasing of the duct section for this venting configuration.

4.CONCLUSIONS

A CFD model based on the unsteady RANS approach for the numerical simulation of a gas explosion vented through a duct has been proposed.

In this model an adjustable parameter is introduced for the calculation of the flame area of the laminar combustion rate. This parameter was previously identified by matching the computed and the experimental pressure of the rear ignition case. The satisfactory agreement between the model results and the experiments has allowed to use the developed CFD code as a numerical tool able to give reliable prediction of the observed experimental trends and it has been then exploited to gain some insights into the phenomenon.

Numerical tests have been carried out by varying the duct geometry i.e. the duct length and diameter. Numerical results have indicated that the trend of increasing pressure with the duct length is to be ascribed to increased pressure losses. Also, with respect to the effect of the duct diameter, it has been observed that larger duct sections are not *a priori* beneficial to relieve the pressure in the vessel, due to the flame distortion effects.

5. REFERENCES

1. NFPA 68, Guide for Venting of Deflagrations, National Fire Protection Association, USA, 2002.
2. R. Siwek, Explosion venting technology, J. Loss Prev. Process Industries 9, 1996, pp. 81-90.
3. W. Bartknecht, Explosions, Course Prevention Protection, 1981, Springer-Verlag, Berlin,.
4. V.V. Molkov, Venting of deflagrations: dynamics of the process in systems with a duct and receiver, Proceedings of the Fourth International Symposium on Fire Safety Science, Canada, 1994, pp. 1245-1254.
5. B. Ponizy, J.C. Leyer, Flame dynamics in a vented vessel connected to a duct: 1. Mechanism of vessel-duct interaction, Combust. Flame 116, 1999, pp. 259-271.
6. B.J. Wiekema, H.J. Pasman, Th.M. Groothuizen, The effect of tubes connected with pressure relief vents, Second International Symposium on Loss Prevention and Safety Promotion in the Process Industries, 1977, pp. 223-231 .

7. W. Kordylewski, J. Wach, Influence of ducting on explosion pressure: small scale experiments, Combust. Flame 71, 1988, pp. 51-61.
8. F. Bouhard, B. Veyssiere, J.C. Leyer, J. Chaineaux, Explosion in a vented vessel connected to a duct, Progress in Astronautics and Aeronautics 134, 1991, pp. 85- 103.
9. B. Ponizy, J.C. Leyer, Flame dynamics in a vented vessel connected to a duct: 2. Influence of ignition site, membrane rupture, and turbulence, Combust. Flame 116, 1999, pp. 272-281.
10. C.J.M. Van Wingerden, J.P. Zeeuwen, On the role of acoustically driven flame instabilities in vented gas explosions and their elimination, Combust. Flame 51, 1983, pp. 109- 111.
11. M.G. Cooper, M. Fairweather, J.P. Tite, On the mechanisms of pressure generation in vented explosions, Combust. Flame 65, 1986, pp. 1- 14.
12. P.A. Cubbage, M.R. Marshall, Pressures generated in combustion chambers by the ignition of air-gas mixtures, IChemE Symposium Series 33, 1972, pp. 24-31.
13. D.P.G. Mc Cann, G.O. Thomas, D.H. Edwards, Gasdynamics of vented explosions Part I: Experimental studies, Comb. Flame 59, 1985, pp. 233-250.
14. D.M. Solberg, J.A. Pappas, E. Skramstad, Observation of flame instabilities in large scale vented gas explosions, Eighteenth Symposium (International) on Combustion, The Combustion Institute, 1981, pp. 1607-1614.
15. R.K. Kumar, W.A. Dewit, D.R. Greig, Vented explosion of hydrogen/air mixtures in a large volume, Combust. Sci. Technol. 66, 1989, pp. 251-266.
16. B. Ponizy, B. Veyssiere, Mitigation of explosions in a vented vessel connected to a duct, Combust. Sci. Technol. 158, 2000, pp.167-182.
17. E.A. Ural, A simplified method for predicting the effect of ducts connected to explosion vents, J. Loss Prev. Process Industries 6, 1993, pp. 3-10.
18. G. Lunn, D. Crowhurst, M. Hey, The effect of vent ducts on the reduced. explosion pressures of vented dust explosions, J. Loss Prev. Process Industries 1, 1988, pp. 182-196.
19. V.V. Molkov, Theoretical generalization of international experimental data on vented explosion dynamics, Proceedings of the First International Seminar on Fire and Explosion Hazard of Substances and Venting of Deflagrations, Moscow, 1995, pp. 166-181.
20. V.V. Molkov, R. Dobashi, M. Suzuki, T. Hirano, Venting of deflagrations: hydrocarbon air and hydrogen-air systems, J. Loss Prev. Process Industries 13, 2000, pp. 397-409.
21. Molkov V.V., Grigorash A.V., Eber R.M., Makarov D.V., Vented gaseous deflagrations: modelling of hinged inertial covers, J. Hazard. Mater. A116, 2004, pp. 1-10.
22. C.J. Lea, H.S. Ledin, A review of the State-of-the-Art in Gas Explosion Modelling, Health and Safety Laboratory, HSL/02, 2002.
23. Salzano E., Marra F.S., Russo G., Lee J.H.S., Numerical simulations of turbulent gas flames in tubes, J. Hazard. Mater. A95, 2002, pp. 233-247.
24. Rigas F., Sklavounos S., Experimentally validated 3-D simulation of shock waves generated by dense explosives in confined complex geometries, J. Hazard. Mater. A121, 2005, pp. 23-30.
25. N.R. Popat, C.A. Catlin, B.J. Arntzen, R.P. Lindstedt, B.H. Hjertager, T. Solberg, O. Saeter, A.C. Van den Berg, Investigations to improve and assess the accuracy of computational fluid dynamic based explosion models, J. Hazard. Mater. 45, 1996, pp. 1-25.
26. P. Naamansen, D. Baraldi, B.H. Hjertager, T., Solberg, R.S. Cant, Solution adaptive CFD simulation of premixed flame propagation over various solid obstructions, J. Loss Prev. Process Industries 15, 2002, pp. 189-197.
27. G. Ferrara, A. Di Benedetto, E. Salzano, G. Russo, CFD analysis of gas explosions vented through relief pipes, to appear in the Journal of Hazardous Materials, 2006
28. CFD-ACE+, CFD Research Corporation, AL (USA), www.cfdrc.com, 2005.
29. B.E Launder, D.B. Spalding, Mathematical Models of Turbulence, 1972, Academic Press, New York,.
30. K.N.C. Bray, The challenge of turbulent combustion, Twenty-sixth Symposium (International) on Combustion, The Combustion Institute,1996, 1-26.

31. J.H. Ferziger, M. Peric, Computational methods for fluid dynamics, 2002, 3Ed., Springer.
32. O. Saeter, Modelling and simulation of gas explosions in complex geometries, Thesis for the Dr. Ing. Degree , University of Bergen, 1998.
33. B.F. Magnussen, B.H. Hjertager, On mathematical modelling of turbulent combustion, Sixteenth Symposium (International) on Combustion, The Combustion Institute,1976, pp. 719-727.
34. K.N.C. Bray, P.A. Libby, Recent developments in the BML model of premixed turbulent combustion, in: Libby, P.A., Williams, F.A. (Eds.), Turbulent Reacting Flows, Academic Press, New York, 1994, pp. 115-151.
35. G.M. Abu-Orf, R.S. Cant, A turbulent reaction rate model for premixed turbulent combustion in spark-ignition engines, Combust. Flame 122, 2000, pp. 233-252.
36. N. Iida, O. Kawaguchi, S. Takeshi, Premixed flame propagating into a narrow channel at a high speed, Part 1: Flame behaviours in the channel, Combust. Flame 60, 1985, pp. 245-255.
37. J.P. Van Doormal, G.D. Raithby, B.H. Mc Donald, The segregated approach to predicting viscous compressible fluid flows, ASME J. Turbomachinery 109, 1987, pp. 268-277.
38. F.P. Lees, Loss Prevention in the Process Industries, Volume 2: Hazard Identification, Assessment and Control, Butterworth Heinemann, 1996.
39. R.P. Benedict, N.A. Carlucci, S.D. Swetz, Flow losses in abrupt enlargements and contractions, J. Eng. Power, Trans. ASME, 88, 1966, pp. 73-81.
40. M.M. Denn , Process Fluid Mechanics, 1980,Prentice-Hall,.
41. D. Bradley, A. Mitcheson A., The venting of gaseous explosions in spherical vessels. I - Theory, Combust. Flame 32, 1978, pp. 221-236.